Nuclear structure study of ^{19,21}N nuclei by γ spectroscopy

Z. Elekes,[1] Zs. Vajta,[1] Zs. Dombrádi,[1] T. Aiba,[2] N. Aoi,[3] H. Baba,[3] D. Bemmerer,[4] Zs. Fülöp,[1] N. Iwasa,[5] Á. Kiss,[6] T. Kobayashi,[5] Y. Kondo,[7] T. Motobayashi,[3] T. Nakabayashi,[7] T. Nannichi,[7] H. Sakurai,[3] D. Sohler,[1] S. Takeuchi,[3] K. Tanaka,[3] Y. Togano,[3] K. Yamada,[3] M. Yamaguchi,[3] and K. Yoneda[3]

[1]*Institute of Nuclear Research of the Hungarian Academy of Sciences, P. O. Box 51, Debrecen, H-4001, Hungary*

[2]*Niigata University, Niigata 950-2181, Japan*

[3]*The Institute of Physical and Chemical Research (RIKEN), 2-1 Hirosawa, Wako, Saitama 351-0198, Japan*

[4]*Forschungszentrum Dresden-Rossendorf, Bautzner Landstrasse 400, D-01328 Dresden (Rossendorf), Germany*

[5]*Tohoku University, Sendai, Miyagi 9808578, Japan*

[6]*Eötvös Loránd University, H-1117 Budapest, Pázmány Péter sétány 1/A, Hungary*

[7]*Tokyo Institute of Technology, 2-12-1 Oh-Okayama, Meguro, Tokyo 152-8551, Japan*

(Received 7 April 2010; revised manuscript received 18 June 2010; published 16 August 2010)

The structure of neutron-rich nitrogen nuclei has been studied by use of neutron removal reaction and inelastic scattering. Mass and charge deformations have been deduced for the first excited state of ^{21}N, which indicates the partial persistence of the $N = 14$ subshell closure in nitrogen isotopes. The spectroscopic information obtained on the structure of ^{19,21}N confirms the results from a previous experiment.

DOI: 10.1103/PhysRevC.82.027305 PACS number(s): 23.20.Js, 25.60.−t, 27.30.+t, 29.30.Kv

I. INTRODUCTION

Because of the proton-neutron monopole interaction, the energies of the single-particle states are changing along an isotopic or isotonic chain by varying the number of neutrons or protons, respectively. As a consequence, shell gaps may disappear, or new shell closures may develop. One of the new subshell closures is at $N = 14$ [1–3], the strength of which was determined to be 4.2 MeV in ^{22}O [4]. Recently, disappearance of this $N = 14$ gap in carbon isotopes has been reported via the spectroscopy of ^{20}C [5]. Also, this observation has been confirmed by the measurement of the mass deformation in ^{20}C [6] in inelastic scattering on a liquid-hydrogen target. Here, as a by-product of the latter experiment, we investigate the interaction of the ^{21}N beam with the hydrogen and lead target, as well. This allowed us to study the transition along the $N = 14$ line and to give spectroscopic information on the structure of the lighter neutron-rich nitrogen isotopes.

II. EXPERIMENTAL DETAILS

The experiment was performed at the Rikagaku Kenkyusho (RIKEN) Nishina Center by using a ^{40}Ar primary beam of 63-MeV/nucleon energy and 700-pnA intensity. The radioactive species were produced through fragmentation reaction on a ^{181}Ta target of 0.2-mm thickness, and their momentum and mass were analyzed by the RIKEN isotope separator (RIPS) [7]. An aluminum wedge degrader of 221-mg/cm^2 thickness was placed at the momentum dispersive focal plane (F1) to purify the secondary beam. RIPS momentum acceptance was set to the maximum value of 6% to achieve the highest intensities because a sharply defined energy was not crucial for our purposes. The resultant beam included several nuclei, mainly ^{17}B, ^{19}C, ^{20}C, ^{21}N, and ^{22}N with a total intensity of about 100 particle/s (pps), to which the contribution of ^{21}N was around 30 pps. The identification of these constituents was carried out event by event by using energy loss (ΔE), time-of-flight (ToF), and magnetic rigidity ($B\rho$) information [8]. A complete separation of the isotopes was achieved by the ΔE-ToF-$B\rho$ method. Two plastic scintillators of 0.3-mm thickness placed at the second and third focal planes (F2 and F3) determined the ToF, while the ΔE value was measured by an Si detector of 0.1-mm thickness at F2. Parallel-plate avalanche counters at F2 and F3 monitored the cocktail beam, which was transported to the secondary targets of ^{208}Pb and liquid hydrogen with 1445-mg/cm^2 and 190-mg/cm^2 thicknesses, respectively. The mean energy of the ^{21}N ions in the middle of the hydrogen and lead target was 52.0 and 48.1 MeV/nucleon. The scattered particles were detected and were identified on the basis of ΔE, ToF, and total energy (E) information. At 80 cm downstream of the target, a plastic scintillator of 1 mm was placed to measure the ΔE and to provide the start signal for the ToF measurement. The end of the ToF signal was determined by an array of plastic detectors located 4.3 m downstream of the target, which also measured the total energy of the isotopes. This array consisted of 16 bars of 60-mm thickness with a total area of 1×1 m^2, and its angular acceptance of 6.5° in the laboratory frame granted almost 100% coverage of the phase space. Some 160 NaI(Tl) crystals of the DALI2 array [9], which surrounded the targets detected the γ rays emitted by the inelastically scattered nuclei. Since knockout reaction channels were strong for the hydrogen target (for the Pb target, this effect was negligible), the separation of the outgoing isotopes was necessary. The atomic number (Z) was well separated by using the ΔE and ToF information, while the mass number (A) was determined on the basis of ToF and total energy (Fig. 1). The mass resolving power for the segments of the plastic scintillator array was different; therefore, only those detectors where the adjacent mass numbers were well resolved were used for the identification of γ rays. However, for the deduction of the cross section of the ^{21}N inelastic scattering reaction, the other detectors, where ^{21}N and ^{20}N were not resolved but ^{21}N was separated well from ^{19}N, were also employed because there are no γ rays with similar energies, which originate from ^{21}N and

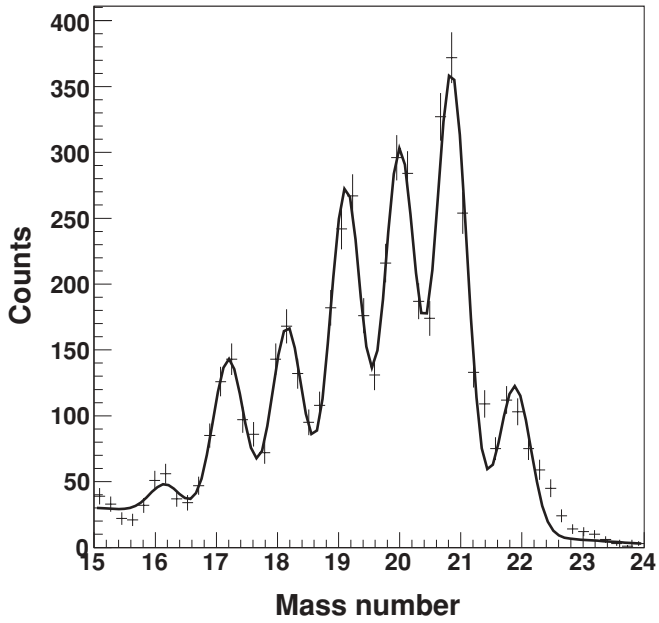

FIG. 1. Linearized mass distribution of nitrogen isotopes from the ^{21,22}N + ^{1}H collision.

^{20}N, but γ rays with energies close to each other are emitted because of transitions in ^{21}N and ^{19}N.

III. RESULTS

A. Level scheme of neutron-rich nitrogen isotopes

The Doppler-corrected spectra, which use the hydrogen target were produced with multiplicity (M) 1 and 2 of the DALI2 array for all the isotopes. Spectra for ^{18}N served as a cross-check of the procedure because the low-energy excited states for this nucleus are well known [10]. By using this information, a GEANT4 [11] simulation of the $M = 1$ and $M = 2$ spectra was performed, and the resulting response curves plus the additional smooth background polynomials fitted the experimental data points well. For the heavier isotopes, the spectra were fitted first by Gaussian functions and polynomial backgrounds to determine the position of the peaks. These were then compared to the γ lines and level scheme found in Ref. [12]. The resulting peaks were fed into the GEANT4 simulation again, the response curves were fitted to the experimental spectra, and the relative intensities were deduced.

Two peaks were found for ^{19}N in the neutron knockout reaction at 529(21) and 1137(26) keV (Fig. 2). This is in good agreement with Ref. [12] where these transitions form a cascade.

For ^{21}N (Fig. 3), the transition between the first excited and ground states [$E_\gamma = 1140(30)$ keV] dominates the proton inelastic scattering spectra with $M = 1$, while the $M = 2$ spectra also contain events, which originate from the transition between the second and first excited states [$E_\gamma = 1210(33)$ keV]. This agrees well with the conclusion drawn in Ref. [12] on the level scheme where the two strongest peaks were found at 1177 and 1228 keV.

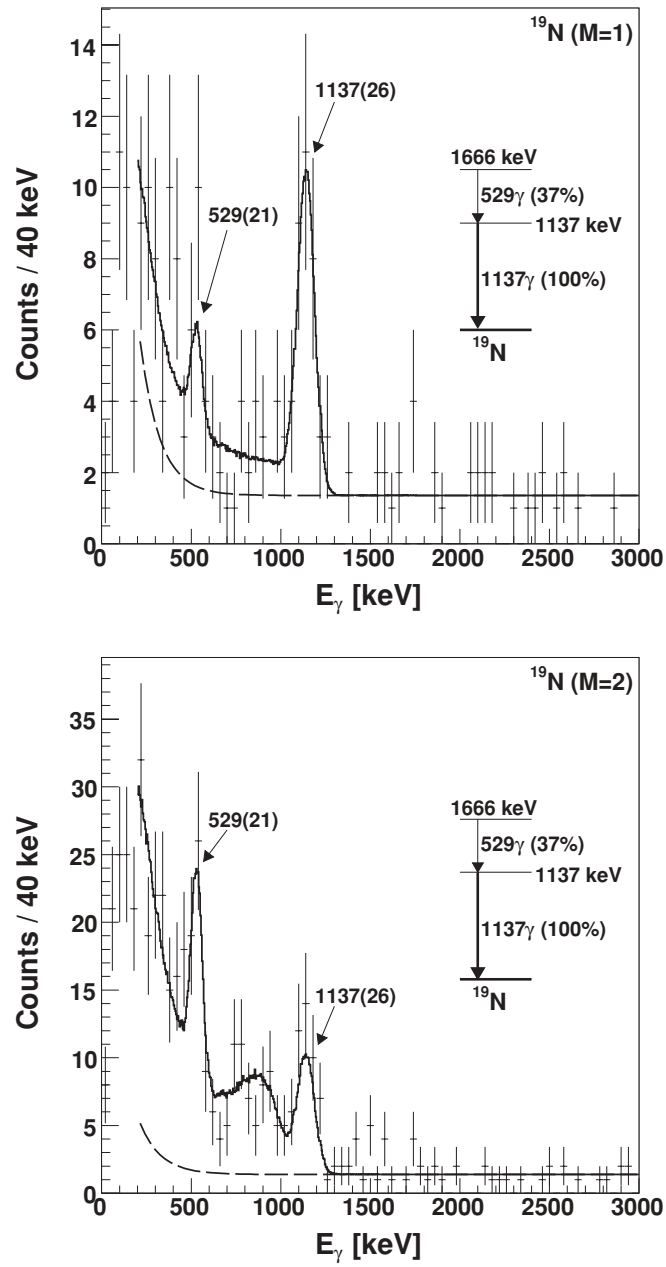

FIG. 2. Doppler-corrected spectra of ^{19}N γ rays, which emerge from neutron knockout reactions with $M = 1$ (upper panel) $M = 2$ (lower panel). The solid line is the final fit, which includes the spectrum curves from the GEANT4 simulation and additional smooth polynomial backgrounds plotted as separate dotted lines.

B. Inelastic scattering cross sections for ^{21}N

In addition to the level scheme, the inelastic scattering cross sections were also deduced for ^{21}N both with hydrogen and with lead targets. The net counts in the nearby peaks for the spectra with liquid hydrogen were derived by fixing the known peak positions and the peak widths determined previously. The relative intensities deduced from the spectrum, which contain all the multipolarities are: 100(10) for the 1140-keV line and 65(6) for the 1210-keV line. The γ feeding of the first excited state was taken into account while the

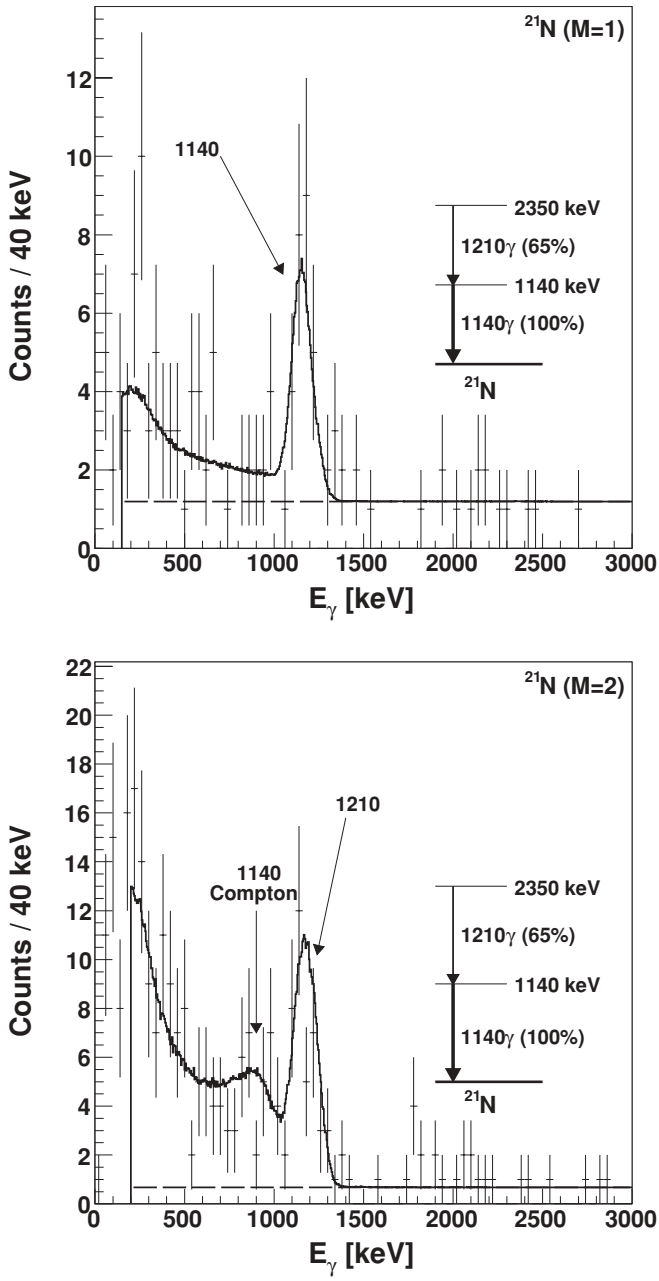

FIG. 3. Doppler-corrected spectra of γ rays, which emerge from the ^{21}N $+^{1}$ H reaction with $M = 1$ (upper panel) and $M = 2$ (lower panel). The solid line is the final fit, which includes the spectrum curves from the GEANT4 simulation and additional smooth polynomial backgrounds plotted as separate dotted lines. The parallel simulation of $M = 1$ and $M = 2$ spectra shows that two peaks (1140 and 1210 keV) are present. Especially, the $M = 2$ spectrum can only be interpreted by assuming the 1210-keV transition, which feeds the first excited state because the GEANT4 curve would otherwise only contain Compton events from the 1140-keV peak.

excitation cross sections were derived. Since only the first excited state was populated in the Pb case and no γ ray was detected in the $M = 2$ spectrum, no correction was taken into account there. The three excitation cross sections determined are $\sigma(1140, \mathrm{H}) = 6.6(8)$ mb, $\sigma(2350, \mathrm{H}) = 12.3(16)$ mb, and $\sigma(1140, \mathrm{Pb}) = 11.4(34)$ mb.

IV. INTERPRETATION AND DISCUSSION

As in several earlier cases (e.g., Ref. [13]), the cross sections were interpreted in terms of the collective model by using the FRESCO code [14]. The optical potential for the hydrogen target was calculated by a parametrized formula from a global phenomenological evaluation [15], while the optical potential determined experimentally in the $^{17}\mathrm{O} + ^{208}\mathrm{Pb}$ reaction [16] was applied to the lead target. The spins of the states involved were taken from shell-model calculations [12] as follows: the ground state has a spin $1/2$, the first excited state at 1140 keV has a spin $3/2$, while the second excited state at 2350 keV has a spin $5/2$.

The determination of the proton and neutron deformation lengths (δ_p,δ_n) was performed in a similar manner described in detail in Ref. [13]; therefore, here, we recall some details. Here, the exception was that the proton inelastic cross section of the second excited state was also available and was used in the χ^2 analysis. As the first step, a pair of neutron and proton deformation lengths has been chosen. These are in the following correspondence with the matter and Coulomb deformation lengths for the two probes ($\delta_M^{\mathrm{Pb}}, \delta_M^{pp}, \delta_C^{\mathrm{Pb}} = \delta_C^{pp} = \delta_p$):

$$\left(Z \cdot b_p^{\mathrm{Pb}} + N \cdot b_n^{\mathrm{Pb}}\right) \cdot \delta_M^{\mathrm{Pb}} = N \cdot b_n^{\mathrm{Pb}} \cdot \delta_n + Z \cdot b_p^{\mathrm{Pb}} \cdot \delta_p, \quad (1)$$

$$\left(Z \cdot b_p^{pp} + N \cdot b_n^{pp}\right) \cdot \delta_M^{pp} = N \cdot b_n^{pp} \cdot \delta_n + Z \cdot b_p^{pp} \cdot \delta_p, \quad (2)$$

where b_n^{Pb}, b_p^{Pb}, b_n^{pp}, and b_p^{pp} are the neutron and proton sensitivity parameters. $\delta_{M,C}^{\mathrm{Pb}}$, $\delta_{M,C}^{pp}$ are the input parameters in the coupled-channel code. The difference between the calculated and the experimental cross sections has been quantified in a χ^2 value, so we ended up with a set of data (δ_n, δ_p, χ^2). This procedure was repeated with varied initial (δ_n, δ_p) parameters, and the results are visualized in a contour plot of χ^2 values (Fig. 4). From this figure, the neutron and proton deformation lengths

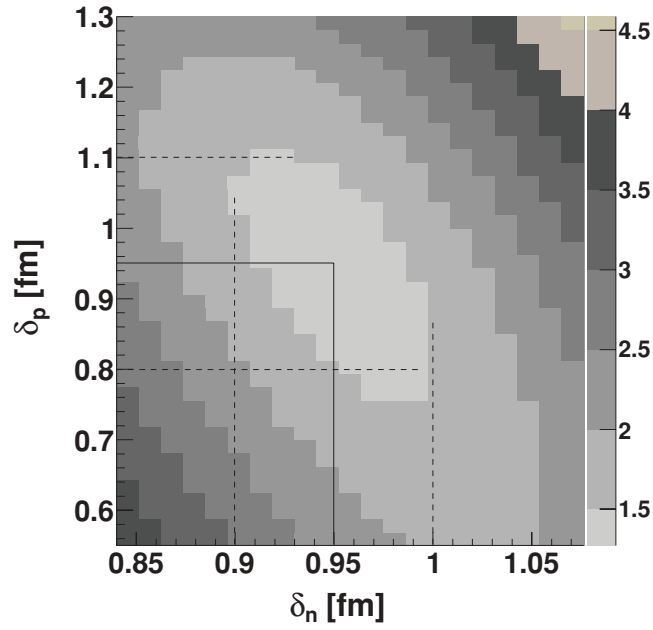

FIG. 4. Contour plot of reduced χ^2 values in a function of the neutron and proton deformation lengths (δ_n, δ_p). The dashed lines represent 1σ error bars.

can easily be determined at $\delta_n = 0.95(5)$ fm, $\delta_p (= \delta_C^{\rm Pb} = \delta_C^{pp}) = 0.95(15)$ fm, which implies $\delta_M^{\rm Pb} = \delta_M^{pp} = 0.95(5)$ fm.

The corresponding reduced electric quadrupole transition probability [$B(E2)$] and the multipole proton and neutron transition matrix elements (M_p, M_n) could be calculated directly with the following formulas:

$$B(E2; 0_{gs}^+ \rightarrow 2_1^+)/e^2 = M_p^2 = \left(\frac{3}{4\pi} \cdot Z \cdot \delta_p \cdot R\right)^2, \quad (3)$$

$$M_n^2 = \left(\frac{3}{4\pi} \cdot N \cdot \delta_n \cdot R\right)^2. \quad (4)$$

With δ_p and δ_n deduced from the fit, we obtain $M_n^2 = 110(12)$ fm^4, $M_p^2 = 28(9)$ fm^4, and the ratio $\frac{M_n}{M_p} = 2.0$ from Eq. (3). This ratio is equal to N/Z, which shows the pure isoscalar character of the transition. These results are similar to those of the ^{22}O nucleus, which has 14 neutrons, just one proton closer to stability [2,3], where small transition matrix elements together with $\frac{M_n}{M_p} = 1.4(5)\frac{N}{Z}$ also were extracted.

According to the weak-coupling approximation [17], the sum of the $E2$ strengths from the ground state to the $3/2^-$ and $5/2^-$ states in the ^{21}N isotope gives the $B(E2; 0^+ \rightarrow 2^+)$ strength in its appropriate core. We have measured the $B(E2)$ value to the first excited state and the mass transition rate to both the first and the second excited states. Since these states mainly are expected to have a $\pi p_{1/2} \oplus 2^+$ nature, it is a good approximation to assume that, for both states, the ratio of the mass and electric transition rates is the same. By using this assumption, the effective $B(E2)$ value of the ground-state transition in the core of ^{21}N can be estimated as $56(18)e^2$ fm^4. The shell-model calculations give $54e^2$ fm^4 summed strength for ^{21}N [12], which is about twice the ^{22}O value and lies about halfway between the neighboring oxygen and carbon $B(E2; 0^+ \rightarrow 2^+)$ values. The shell-model calculation gives $110e^2$ fm^4 for ^{20}C, which is much larger than the experimental value ($<18e^2$ fm^4) because of the decoupling of the neutrons from the core in heavy carbon nuclei [6]. This fact shows that the core structure of the nitrogen isotopes is softer than that of the singly closed-shell oxygen isotopes and is consistent with the 1.2-MeV reduction of the $N = 14$ shell closure when going from ^{22}O to ^{21}N as a result of the removal of a proton from the $p_{1/2}$ orbit [12].

ACKNOWLEDGMENTS

We thank the RIKEN Ring Cyclotron staff for their assistance during the experiment. One of the authors (Z. E.) is grateful for the Bolyai grant from Hungary. The European authors acknowledge the kind hospitality and support from RIKEN. The present work was partly supported by the Grant-in-Aid for Scientific Research (No. 1520417) by the Ministry of Education, Culture, Sports, Science and Technology and by OTKA Grants No. K68801, No. T049837, and No. NKTH JP-16/2006.

[1] P. G. Thirolf, Phys. Lett. B **485**, 16 (2000).
[2] E. Becheva *et al.*, Phys. Rev. Lett. **96**, 012501 (2006).
[3] Z. Elekes *et al.*, Phys. Rev. C **74**, 017306 (2006).
[4] M. Stanoiu *et al.* Phys. Rev. C **69**, 034312 (2004).
[5] M. Stanoiu *et al.* Phys. Rev. C **78**, 034315 (2008).
[6] Z. Elekes *et al.* Phys. Rev. C **79**, 011302 (2009).
[7] T. Kubo *et al.*, Nucl. Instrum. Methods B **70**, 309 (1992).
[8] H. Sakurai *et al.*, Phys. Lett. B **448**, 180 (1999).
[9] S. Takeuchi *et al.*, RIKEN Accel. Prog. Rep. **36**, 148 (2003).
[10] M. Wiedeking *et al.*, Phys. Rev. C **77**, 054305 (2008).
[11] S. Agostinelli *et al.*, Nucl. Instrum. Methods A **506**, 250 (2003).
[12] D. Sohler *et al.*, Phys. Rev. C **77**, 044303 (2008).
[13] Z. Elekes *et al.*, Phys. Rev. C **78**, 027301 (2008).
[14] I. J. Thompson [www.fresco.org.uk].
[15] A. J. Koning *et al.*, Nucl. Phys. A **713**, 231 (2003).
[16] J. Barrette *et al.*, Phys. Lett. B **209**, 182 (1988).
[17] K. Alder, Rev. Mod. Phys. **28**, 432 (1956).